INTERNATIONAL JOURNAL FOR NUMERICAL METHODS IN ENGINEERING
Int. J. Numer. Meth. Engng 2012; **91**:450–456
Published online 1 June 2012 in Wiley Online Library (wileyonlinelibrary.com). DOI: 10.1002/nme.4290

Stable time step estimates for mesh-free particle methods

Grand Roman Joldes*,†, Adam Wittek and Karol Miller

Intelligent Systems for Medicine Laboratory, School of Mechanical and Chemical Engineering, The University of Western Australia, 35 Stirling Highway, Crawley/Perth WA 6009, Australia

SUMMARY

Real-time computational biomechanics for medicine usually uses explicit time integration, because of its efficiency and suitability for parallel implementation. Explicit time integration is only conditionally stable and therefore requires an estimation of the maximum stable time step that can be used. In this paper we develop a method of estimating the stable time step for mesh-free particle methods for a specific case of mass lumping: the mass associated with an integration point is distributed equally to all nodes found in the support domain of that integration point. Two estimates of the stable time step for each integration point are developed: one that is very accurate but more costly to compute and one less accurate but easier to implement. The results are also valid for the FEM and beyond computational biomechanics for medicine.
Copyright © 2012 John Wiley & Sons, Ltd.

Received 10 June 2011; Revised 9 January 2012; Accepted 11 January 2012

KEY WORDS: stability analysis; stable time step; mesh-free particle methods; maximum eigenvalue estimation

1. INTRODUCTION

In the past few years our research group developed a suite of finite element algorithms for computing soft tissue deformation based on the total Lagrangian formulation and using explicit time integration [1–4]. By using artificial mass proportional damping in the explicit integration schemes, such algorithms can not only be used for time accurate simulations, but also for fast computation of the steady state solution [5, 6]. Parallel implementations of these algorithms lead to real-time performance for intra-operative brain shift computations using comprehensive finite element models having more than 50,000 DOFs and including different element types, nonlinear materials, large deformations and contacts [7].

While applying these algorithms for intraoperative image registration [8, 9], some important weakness of the FEM became evident:

- To obtain good results and convergence of the simulation, a good quality mesh is needed. Such mesh is very hard to build for complicated organ shapes (such as the brain), and automatic generation is almost impossible for any element type except tetrahedrons.
- Even if a good quality mesh is used, the solution method may still fail in case of large deformations, because of problems such as element inversion.

To circumvent these problems, we considered the use of mesh-free methods, such as the mesh-free total Lagrangian explicit dynamics algorithm based on the element free Garlekin method [10]. Such methods do not require a good quality mesh to be generated, because the shape functions are constructed based on a cloud of points, and they also perform much better in case of very large

*Correspondence to: Grand Roman Joldes, School of Mechanical and Chemical Engineering, The University of Western Australia, 35 Stirling Highway, Crawley/Perth WA 6009, Australia.

†E-mail: grandj@mech.uwa.edu.au

Copyright © 2012 John Wiley & Sons, Ltd.

deformations. Therefore, we propose to use mesh-free methods combined with explicit solution algorithms for more robust surgical simulations.

Explicit time integration can be used to perform dynamic simulations, leading to time accurate solutions, or for quasi-static simulations, to obtain the steady state solution. Because it does not require the solution of large systems of equations, explicit integration can be much more computationally efficient at finding the solution than other methods (implicit integration, static analysis). It also leads to solution algorithms that can be easily implemented on parallel hardware such as graphics processing units [7]. The main disadvantage of explicit integration is its conditional stability — the time step used for time integration must be smaller than a critical time step for the solution to converge [11].

In the case of the FEM there are well established formulae for estimating the critical time step for each element type [11, 12]. These formulae are generally developed using the assumption of a homogenous isotropic material.

For mesh-free particle methods, there are few available methods for estimating the critical time step, and these methods are not generally valid. In [13] Belytschko *et al.* developed critical time step bounds for one-dimensional and two-dimensional (2D) mesh-free methods. Nevertheless, these bounds are valid in 2D only for uniformly distributed nodes, and they cannot be used for shape functions that have the Kronecker delta property and for shape functions that are not strictly positive, because they become indefinite (because of division by zero) [14]. Puso *et al.* presented in [14] an estimation of the critical time step for nodal integration methods. This estimation also uses the assumption of a homogenous material. Benson presented an algorithm that produces an accurate estimate of the critical time step in the context of the FEM [15], which can be easily adapted for mesh-free methods. The algorithm proposed by Benson uses an iterative method called 'power iteration' to estimate the maximum eigenvalue of the assembled system of equations.

The critical time step is directly related to the maximum frequency of free vibration, which is determined by the mass and stiffness matrices of the system. Therefore, different lumping techniques used for obtaining a diagonal mass matrix lead to different critical time steps for the system. In this paper we consider that the mass associated with an integration point is distributed equally to all nodes found in the support domain of that integration point. The lumping technique has no influence on the results of a steady state analysis [6], because the mass matrix does not influence the steady state solution (for elastic materials). The correctness of results can be influenced by the mass lumping technique in case of dynamic analysis; therefore, the analyst must check whether our specific lumping technique is appropriate for a given problem when such analysis is performed.

In the next section we develop a new method for estimating the critical time step for a mesh-free particle method. In Section 3 we assess the performance of the new method and Section 4 contains discussions and conclusions.

2. CRITICAL TIME STEP ESTIMATION

We consider a mesh-free particle method for which the displacement field is approximated by

$$\mathbf{u}(\mathbf{x}) = \sum_{I \in N(\mathbf{x})} h_I(\mathbf{x}) \cdot \mathbf{u}^I, \tag{1}$$

where $\mathbf{u}^I$ are the field variable values at node I, $N(\mathbf{x})$ is the set of nodes in the support domain of $\mathbf{x}$ and h_I is the shape function for node I.

The matrix of shape function derivatives is defined as

$$\mathbf{B}_{jI}(\mathbf{x}) = \frac{\partial h_I(\mathbf{x})}{\partial x_j}. \tag{2}$$

The stable critical time step for central difference integration can be obtained from the maximum frequency of free vibration as [16]

$$\Delta t^{\text{crit}} = \frac{2}{\omega_{\max}}. \tag{3}$$

Copyright © 2012 John Wiley & Sons, Ltd.

DOI: 10.1002/nme

Similar formulae are available for other explicit time integration methods [11].

The mass and stiffness matrices for the system are obtained by assembling the corresponding matrices from each integration point

$$\mathbf{K} = \sum_{I=1}^{N} \mathbf{K}^I \tag{4}$$

$$\mathbf{M} = \sum_{I=1}^{N} \mathbf{M}^I, \tag{5}$$

where N is the number of integration points.

The maximum free vibration frequency of the assembled system can be estimated using the eigenvalue inequality theorem [17]

$$\min_I \left(\lambda^I_{\text{Min}}\right) \leq \lambda_{\text{Min}} \leq \lambda_{\text{Max}} \leq \max_I \left(\lambda^I_{\text{Max}}\right) \tag{6}$$

Therefore, a conservative estimate of the critical time step for the central difference method is given by

$$\Delta t_{\text{crit}} = \frac{2}{\omega_{\max}} = \frac{2}{\sqrt{\lambda_{\max}}} \approx \frac{2}{\sqrt{\max_I(\lambda^I_{\text{Max}})}} = \min_I \left(\frac{2}{\sqrt{\lambda^I_{\text{Max}}}}\right) = \min_I \left(\Delta t^I_{\text{crit}}\right). \tag{7}$$

For a given integration point, the maximum eigenvalue can be estimated using the Rayleigh quotient as [17]

$$\lambda^I_{\text{Max}} = \sup_{\mathbf{u}} \frac{\mathbf{u}^T \mathbf{K}^I \mathbf{u}}{\mathbf{u}^T \mathbf{M}^I \mathbf{u}}. \tag{8}$$

Considering our specific mass lumping technique (mass associated to an integration point is distributed equally to all nodes found in the support domain of that integration point), the above relation can be rewritten as

$$\lambda^I_{\text{Max}} = \frac{N^I}{m^I} \sup_{\mathbf{u}} \frac{\mathbf{u}^T \mathbf{K}^I \mathbf{u}}{\mathbf{u}^T \mathbf{u}} = \frac{N^I}{m^I} \rho_{\text{Max}}(\mathbf{K}^I), \tag{9}$$

where N^I is the number of nodes in the support domain of integration point I, m^I is the mass allocated to integration point I and $\rho_{\text{Max}}(\mathbf{K}^I)$ is the maximum eigenvalue of the stiffness matrix for integration point I.

The stiffness matrix for integration point I is defined as

$$\mathbf{K}^I_{iJlK} = \mathbf{B}_{jJ}(\mathbf{x}^I)\mathbf{C}_{ijkl}\mathbf{B}_{lK}(\mathbf{x}^I) \cdot V^I = \mathbf{B}^I_{jJ}\mathbf{C}_{ijkl}\mathbf{B}^I_{lK} \cdot V^I, \tag{10}$$

where V^I is the volume allocated to integration point I [14]. For a homogenous isotropic material, the maximum eigenvalue of the stiffness matrix is developed in [14] as

$$\rho_{\text{Max}}(\mathbf{K}^I) \leq \left(\lambda \left\|\mathbf{B}^I\right\|^2_{\text{F}} + 2\mu \cdot \left\|\mathbf{B}^I\right\|^2_2\right) \cdot V^I \leq (\lambda + 2\mu) \cdot V^I \cdot \left\|\mathbf{B}^I\right\|^2_{\text{F}}, \tag{11}$$

where λ and μ are the Lame constant, $\|B\|_F$ is the Frobenious norm

$$\left\|\mathbf{B}\right\|^2_{\text{F}} = \mathbf{B}_{jI}\mathbf{B}_{jI} \tag{12}$$

and $\|B\|_2$ is the matrix spectral norm, defined as

$$\left\|\mathbf{B}\right\|^2_2 = \rho_{\text{Max}}(\mathbf{B}_{iJ}\mathbf{B}_{jJ}). \tag{13}$$

Copyright © 2012 John Wiley & Sons, Ltd.

DOI: 10.1002/nme

By substituting (11) in (9), and considering the definition of density, we get the bounds for the maximum eigenvalues of the stiffness matrix as

$$\lambda^I_{\text{Max}} \leqslant \frac{N^I}{\rho^I}\left(\lambda \mathbf{B}^I_{jI}\mathbf{B}^I_{jI} + 2\mu \cdot \rho_{\text{Max}}(\mathbf{B}^I_{iJ}\mathbf{B}^I_{jJ})\right) \tag{14}$$

$$\lambda^I_{\text{Max}} \leqslant \frac{N^I}{\rho^I}(\lambda + 2\mu) \cdot \left\|\mathbf{B}^I\right\|^2_F = N^I c^{I2} \cdot \mathbf{B}^I_{jI}\mathbf{B}^I_{jI}, \tag{15}$$

where ρ is the material density and c is the dilatational wave speed. These can be used directly in Equation (7) for estimating the critical time step. Although Equation (14) offers a better estimate, it involves the computation of the maximum eigenvalue of a 3×3 matrix (in 3D), and therefore Equation (15) may be preferred in practice.

The bounds for the maximum eigenvalue of the stiffness matrix, as given by Equations (14) and (15), are valid for one-dimensional, 2D and 3D cases. They are also valid for finite elements, as long as the same mass lumping technique is used. For the uniform strain hexahedron and quadrilateral these bounds give the same result as the ones presented in [12].

3. PERFORMANCE EVALUATION

To evaluate the performance of our algorithm for the critical time step estimation for different numbers of nodes per integration point, we use the nodal distribution presented in Figure 1 for a 2D case and in Figure 4 for a 3D case. For each node we define an influence domain based on the local node density. We use a dense grid of regularly distributed integration points to get different nodes-integration points associations. For the chosen parameters, we have between 3 and 11 nodes associated with an integration point in 2D. We compute the moving least squares (MLS) shape functions and their derivatives (matrix **B**, see Equation (2)) at each integration point. Using the **B** matrix we can compute the stiffness matrix (Equation (10)), find its maximum eigenvalue and compute the real value of the critical time step for a given integration point. We can compare the actual value of the critical time step with estimates computed using Equations (14) and (15). The obtained results are presented in Figure 2 for a plane strain analysis and in Figure 3 for a plane stress analysis.

The obtained results show that Equation (14) leads to a very good critical time step estimate, which is less than 5% lower than the actual value, for the entire range considered for the material's Poisson's ratio. The estimate of the critical time step given by Equation (15) can be as much as 30% lower than the actual value, with a better prediction for higher values of the material's Poisson's

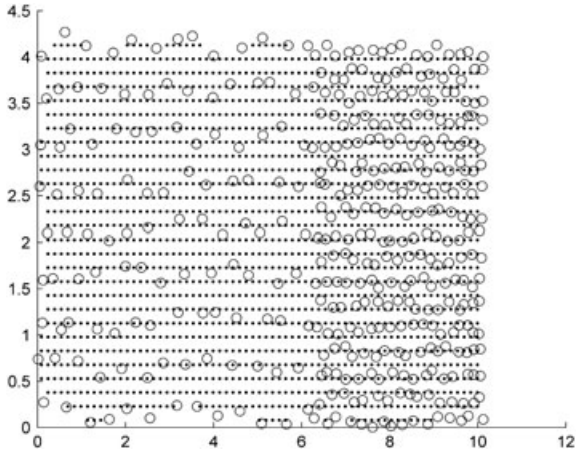

Figure 1. The distribution of nodes (represented by circles) and integration points used for performance evaluation. MLS shape functions are computed for each integration point.

Copyright © 2012 John Wiley & Sons, Ltd.

DOI: 10.1002/nme

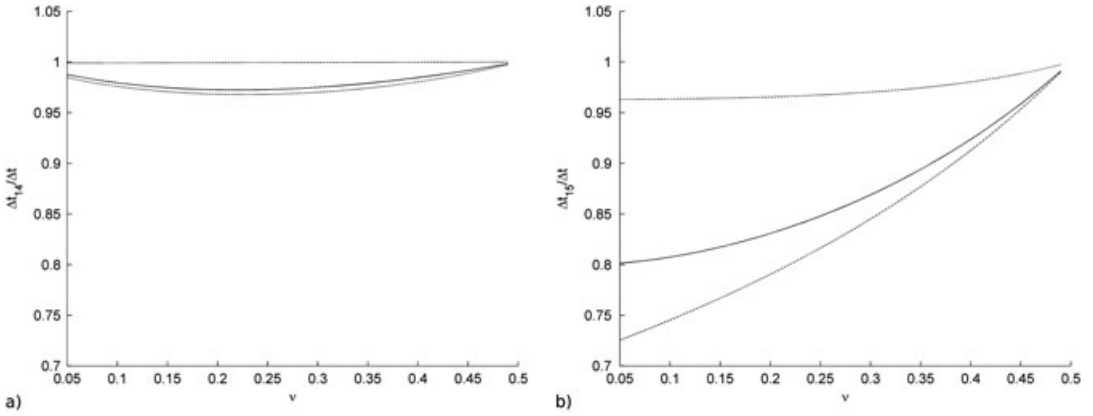

Figure 2. The ratio of critical time step estimates, as given by Equations 14 (a) and 15 (b), to the real critical time step obtained based on the stiffness matrix is computed for all integration points. The maximum, minimum (dotted lines) and average values (solid line) of these ratios are plotted against material's Poisson's ratio, for a plane strain analysis.

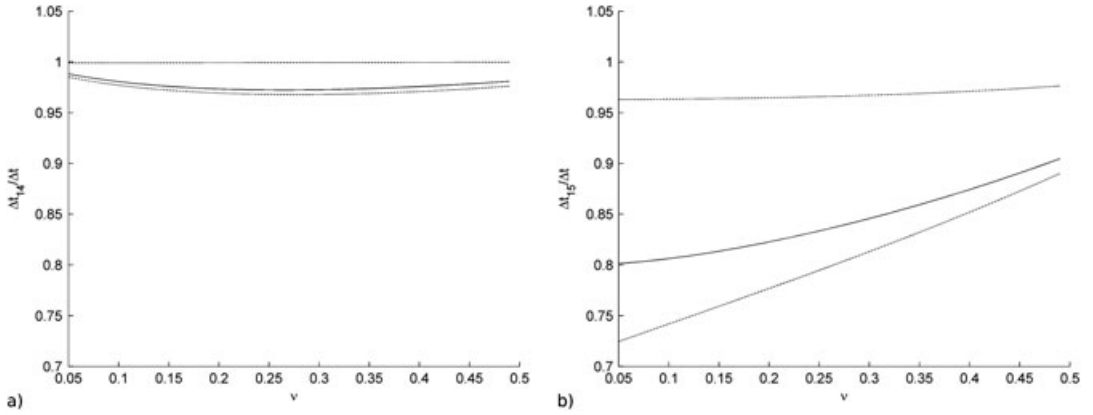

Figure 3. The ratio of critical time step estimates, as given by Equations 14 (a) and 15 (b), to the real critical time step obtained based on the stiffness matrix is computed for all integration points. The maximum, minimum (dotted lines) and average values (solid line) of these ratios are plotted against material's Poisson's ratio, for a plane stress analysis.

ratio. Also the estimate given by Equation (15) is better for plane strain than for plane stress analyses, especially at higher values of the material's Poisson's ratio.

We performed a similar evaluation for 3D shape functions using the nodes and integration points distributed as in Figure 4, with a variable nodal influence domain leading to between 8 and 25 nodes associated to an integration point. The obtained results are presented in Figure 5. The obtained results for 3D are very similar with those obtained for a plane strain analysis in 2D.

4. DISCUSSION AND CONCLUSSIONS

In this paper we presented a method for estimating the critical time step for mesh-free particle methods. The estimates are valid for a specific case of mass lumping: the mass associated with an integration point is distributed equally to all nodes found in the support domain of that integration point. The same estimation method can also be used for finite elements if the mass lumping is done in the same way.

We presented two formulas that can be used for estimating the critical time step. These formulas were obtained considering a homogenous isotropic material and are valid both in 2D and 3D. The first formula (Equation (14)) leads to a very good estimate, for any value of the material's Poisson's

Copyright © 2012 John Wiley & Sons, Ltd.

DOI: 10.1002/nme

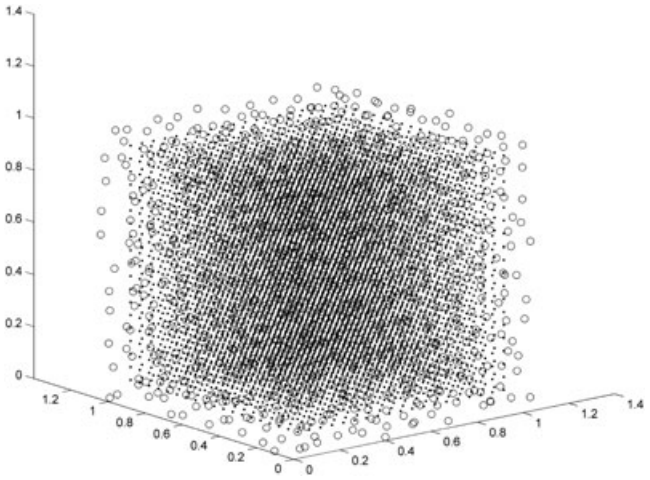

Figure 4. The distribution of nodes (represented by circles) and integration points used for performance evaluation in 3D. MLS shape functions are computed for each integration point.

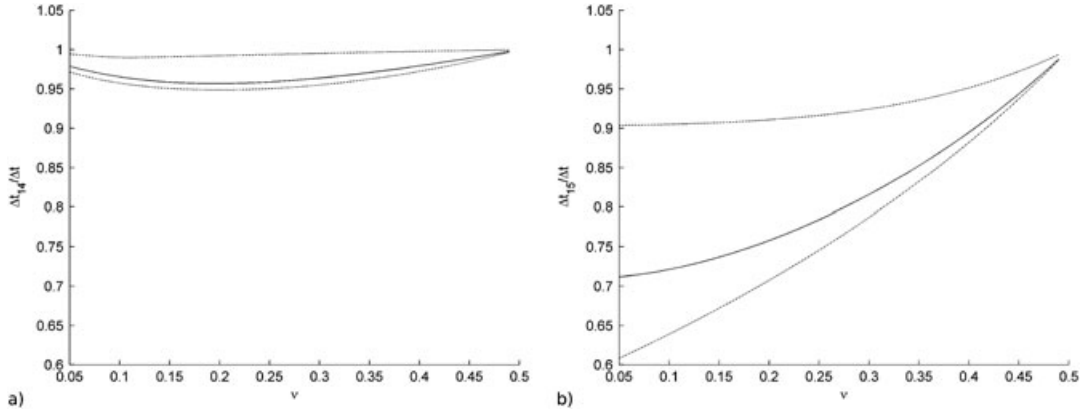

Figure 5. The ratio of critical time step estimates, as given by Equations 14 (a) and 15 (b), to the real critical time step obtained based on the stiffness matrix is computed for all integration points. The maximum, minimum (dotted lines) and average values (solid line) of these ratios are plotted against material's Poisson's ratio, for a 3D analysis.

ratio, but it requires the computation of the maximum eigenvalue of a 2×2 (2D) or 3×3 (3D) matrix. The second formula (Equation (15)) is much simpler, but the accuracy of the estimates it provides is lower, especially for materials with a low Poisson's ratio. Nevertheless, this might be a better option for a large deformation nonlinear solver implementation, because the critical time step might decrease during the analysis (because of changes in nodal positions and material properties because of the large deformations). The second formula would also be a good choice for almost incompressible materials, such as brain tissue, which have a very large Poisson's ratio.

As shown by the eigenvalue inequality theorem (6), the estimates presented in this paper, based on the maximum eigenvalues at integration points, underestimate the critical time step. Although beneficial for the convergence of the explicit integration scheme, such underestimate leads to more time steps needed for analysis, and therefore more computational effort. The algorithm proposed by Benson in [15] produces a more accurate estimate of the critical time step. Unfortunately, the 'power iteration' procedure used by Benson approaches the maximum eigenvalue from below and therefore needs to be almost converged before using it to calculate the critical time step. Benson also proposed to combine his accurate (but computationally intensive) algorithm with element-based time step estimates to obtain a good estimate of the critical time step at a lower computational cost

Copyright © 2012 John Wiley & Sons, Ltd.

DOI: 10.1002/nme

(the accurate algorithm is used every few time steps to improve the critical time step prediction). In a mesh-free setting, the algorithm proposed by Benson can be combined with the formulae developed in this paper. Nevertheless, the number of steps between updates of the critical time step using Benson's more accurate algorithm seems to be problem dependent, and for some problems the update is needed at every time step [15]. The above shortcomings limit the usefulness of Benson's algorithm to specific problems. The formulae presented in this paper seem to offer a sufficiently accurate critical time step prediction in most situations.

The developed formulas offer a way of estimating the critical time step for mesh-free methods, which can then be used together with explicit time integration algorithms to solve computational biomechanics problems in real time. Although developed in the context of linear elasticity, empirical evidence from the use of similar formulae with the FEM suggests that these formulae are also useful for simulations involving large deformations and nonlinear material models [11].

ACKNOWLEDGEMENTS

The financial support of the Australian Research Council (Grant No. DP1092893) and NHMRC (Grant No. 1006031) are gratefully acknowledged.

REFERENCES

1. Miller K, Joldes GR, Lance D, Wittek A. Total lagrangian explicit dynamics finite element algorithm for computing soft tissue deformation. *Communications in Numerical Methods in Engineering* 2007; **23**:121–134.
2. Joldes GR, Wittek A, Miller K. An efficient hourglass control implementation for the uniform strain hexahedron using the total lagrangian formulation. *Communications in Numerical Methods in Engineering* 2008; **24**:1315–1323.
3. Joldes GR, Wittek A, Miller K. Non-locking tetrahedral finite element for surgical simulation. *Communications in Numerical Methods in Engineering* 2009; **25**:827–836.
4. Joldes GR, Wittek A, Miller K. Suite of finite element algorithms for accurate computation of soft tissue deformation for surgical simulation. *Medical Image Analysis* 2009; **13**:912–919.
5. Joldes GR, Wittek A, Miller K. Computation of intra-operative brain shift using dynamic relaxation. *Computer Methods in Applied Mechanics and Engineering* 2009; **198**:3313–3320.
6. Joldes GR, Wittek A, Miller K. An adaptive dynamic relaxation method for solving nonlinear finite element problems. Application to brain shift estimation. *International Journal for Numerical Methods in Biomedical Engineering* 2011; **27**:173–185.
7. Joldes GR, Wittek A, Miller K. Real-time nonlinear finite element computations on GPU - application to neurosurgical simulation. *Computer Methods in Applied Mechanics and Engineering* 2010; **199**:3305–3314.
8. Wittek A, Joldes GR, Couton M, Warfield SK, Miller K. Patient-specific non-linear finite element modelling for predicting soft organ deformation in real-time; Application to non-rigid neuroimage registration. *Progress in Biophysics and Molecular Biology* 2010; **103**:292–303.
9. Miller K, Wittek A, Joldes GR, Horton A, Roy TD, Berger J, Morriss L. Modelling brain deformations for computer-integrated neurosurgery. *International Journal for Numerical Methods in Biomedical Engineering* 2010; **26**:117–138.
10. Horton A, Wittek A, Joldes GR, Miller K. A meshless total lagrangian explicit dynamics algorithm for surgical simulation. *International Journal for Numerical Methods in Biomedical Engineering* 2010; **26**:977–998.
11. Belytschko T. An overview of semidiscretization and time integration procedures. In *Computational Methods for Transient Analysis*, Belytschko T, Hughes TJR (eds). Elsevier: Amsterdam, 1983; 1–65.
12. Flanagan DP, Belytschko T. Eigenvalues and stable time steps for the uniform strain hexahedron and quadrilateral. *Journal of Applied Mechanics* 1984; **51**:35–40.
13. Belytschko T, Guo Y, Liu WK, Xiao SP. A unified stability analysis of meshless particle methods. *International Journal for Numerical Methods in Engineering* 2000; **48**:1359–1400.
14. Puso MA, Chen JS, Zywicz E, Elmer W. Meshfree and finite element nodal integration methods. *International Journal for Numerical Methods in Engineering* 2008; **74**:416–446.
15. Benson DJ. Stable time step estimation for multi-material eulerian hydrocodes. *Computer Methods in Applied Mechanics and Engineering* 1998; **167**:191–205.
16. Belytschko T, Liu KW, Moran B. *Nonlinear Finite Elements for Continua and Structures*. John Wiley & Sons Ltd: Chichester, 2006.
17. Bathe K-J. *Finite Element Procedures*. Prentice-Hall: New Jersey, 1996.

Copyright © 2012 John Wiley & Sons, Ltd.

DOI: 10.1002/nme